16th World Conference on Earthquake Engineering, 16WCEE 2017

Santiago Chile, January 9th to 13th 2017

Paper N° 4273

Registration Code: S-R1464692017

THE 2015 GORKHA EARTHQUAKE SEQUENCE: STRONG GROUND MOTION FEATURES

R. Rupakhety[(1)], S. Ólafsson[(2)], B. Halldorsson[(3)]

[(1)] *Associate Professor, Earthquake Engineering Research Centre, University of Iceland, rajesh@hi.is*
[(2)] *Research Professor, Earthquake Engineering Research Centre, University of Iceland, simon@hi.is*
[(3)] *Research Professor, Earthquake Engineering Research Centre, University of Iceland, skykkur@hi.is…*

Abstract

The 2015 Gorkha Earthquake and its aftershocks caused a major disaster in Nepal causing widespread casualties, injuries, and physical damage. Ground motion from the mainshock and the largest aftershocks recorded at Kathmandu Valley are studied in detail in this contribution. Horizontal ground motion due to the mainshock has a very peculiar energy content, with spectral ordinates as high as 0.5g at a period of about 5s. while peak ground acceleration is relative low at around 16% of acceleration of gravity. This implies an amplification factor of about 3 at a vibration period of 5s, which is 10 times larger than that implied by modern design codes such as the Eurocode 8. Spectral shapes of horizontal and vertical motion due to the mainshock and the aftershocks are very poorly represented by those recommended in modern design codes as well as uniform hazard spectral shapes obtained from standard probabilistic seismic hazard assessment. Although peak ground acceleration is slightly larger in the vertical motion than in the horizontal motion, peak ground velocity is much larger in horizontal motion. This indicates higher frequency content in vertical motion than in the horizontal motion, partly due to possibly the effects of soft and deep sediments of the valley which damped out high-frequency motion but amplified the lower frequencies. Although ground motion is available until now at only one station in Kathmandu Valley, careful examination of the available data provides a lot of insight into its nature. The most important insight being the fact that standard design spectra recommended in modern codes greatly underestimate spectral ordinates at periods of vibration longer than about 0.5s. This has a serious consequence that use of such spectral shapes for design of high-rise buildings in the Valley may result in serious under-estimation of expected seismic action. It is also apparent that uniform hazard spectra based on ground motion prediction models calibrated from data recorded elsewhere are not applicable in the Valley. These observations necessitate development of suitable ground motion models as well as geotechnical site response models. The results indicate that high-rise (more than about 5 storeys tall) buildings in the Valley should be very carefully designed. Until proper ground-motion models are calibrated a lot of uncertainties exists in the seismic action expected in such structures during future earthquakes.

Keywords: Gorkha Earthquake, response spectra, strong ground motion, coseismic displacement

1. Introduction

A strong earthquake struck Nepal on 25 April 2015 at 11:26 UTC (local time 11:56). United States Geological Survey (USGS) located the epicentre (see red star in Fig. 1) of the earthquake about 77 km North-West of Kathmandu, near Barpak Village in Gorkha district [1]. The epicentre located by National Seismological Centre (NSC) of Department of Mines and Geology of Government of Nepal [2] is close by (see white star in Fig. 1) that located by USGS, while the Global CMT [3] locates it close to Kathmandu. The size of the earthquake was estimated to be moment magnitude 7.8 by USGS and local magnitude 7.6 by NSC. Several strong aftershocks followed the earthquake, the largest of them being the 12 May Mw 7.3 earthquake [1] which occurred east of Kathmandu.

The Gorkha Earthquake is the largest natural disaster to affect Nepal since 1934 when a devastating Mw 8.1 earthquake struck the country. As of 21 June 2015, 8795 casualties and 22310 injuries have been confirmed [4]. According to [4], 799062 buildings have been affected of which 284352 have been completely damaged and 514710 have been partially damaged. Of the affected buildings, 6278 host government offices while the rest are privately owned. The most severely affected districts are Sindhupalchok, Kathmandu, Nuwakot, Dhading, and Rasuwa.

The district wise distribution of casualties, injuries, and damage to buildings are shown in Fig. 1. In Sindhupalchock alone, 3440 (~39% of all casualties) people died while 1223, 1101, 733, and 660 casulties have been reported in Kathmandu, Nuwakot, Dhading, and Rasuwa, respectively. Very few instances of death (~6) have been reported west of Kaski district which lies to the west of the mainshock epicenter. Injuries were sustained by people in most of the districts (see Fig. 2b). In Kathmandu, Lalitpur, Bhaktapur, Sinddhupalchok, and Dhading about 7949, 3052, 2101, 1573, and 1218 people were injured, respectively. In total, 22311 people have been reported injured.

Ground shaking due to the earthquake caused damage to buildings in most of the country (see Fig. 2c and 2d). More than 95% of buildings have been completely damaged in Sindhupalchok, Dolakha, and Nuwakot. In Kathmandu district, ~8.5% of buildings have been completely damaged while ~11.7% have been partially damaged. It is interesting to note that casualties, injuries, and complete collapse of buildings are concentrated in the area between the mainshock and the largest aftershock. The geographical area with high percentage of complete collapse of buildings (see Figure 1c) matches very well with the fault planes of the two events as estimated by USGS [1]. It is also noteworthy that the districts east of the epicenter are affected more than those to the west. This is because of larger intensity of ground shaking in these districts as they lie above the fault plane and the rupture on the fault plane propagated towards east causing strong directivity effects. High level of damage in Sindhupalchok, Dolakha and neighbouring districts east and north of Kathmandu is partially due to the 12 May 2015 aftershock which collapsed many buildings that were partially damaged by the mainshock.

2. The 25 April mainshock and its aftershocks

The magnitude of the 25 April Earthquake was reported as 7.8 Mw by the USGS [1]. The local magnitude Ml reported for the event by NSC [2] was 7.6. This difference is natural owing to the different scales used by the two agencies, however, the reported local magnitude of 7.6 is unusual as the local scale, in general, is found to saturate at about 6.9. In this context, we find it useful to investigate the relation between the moment magnitude and local magnitude for the Gorkha Earthquake and its aftershocks. This would allow a comparison of the relation between these two scales for the Gorkha Earthquake with similar relations reported for other earthquakes. Furthermore, it would allow us to convert the magnitude reported by NSC to Mw, so that a consistent magnitude scale can be used to study the temporal characteristics of the aftershocks.

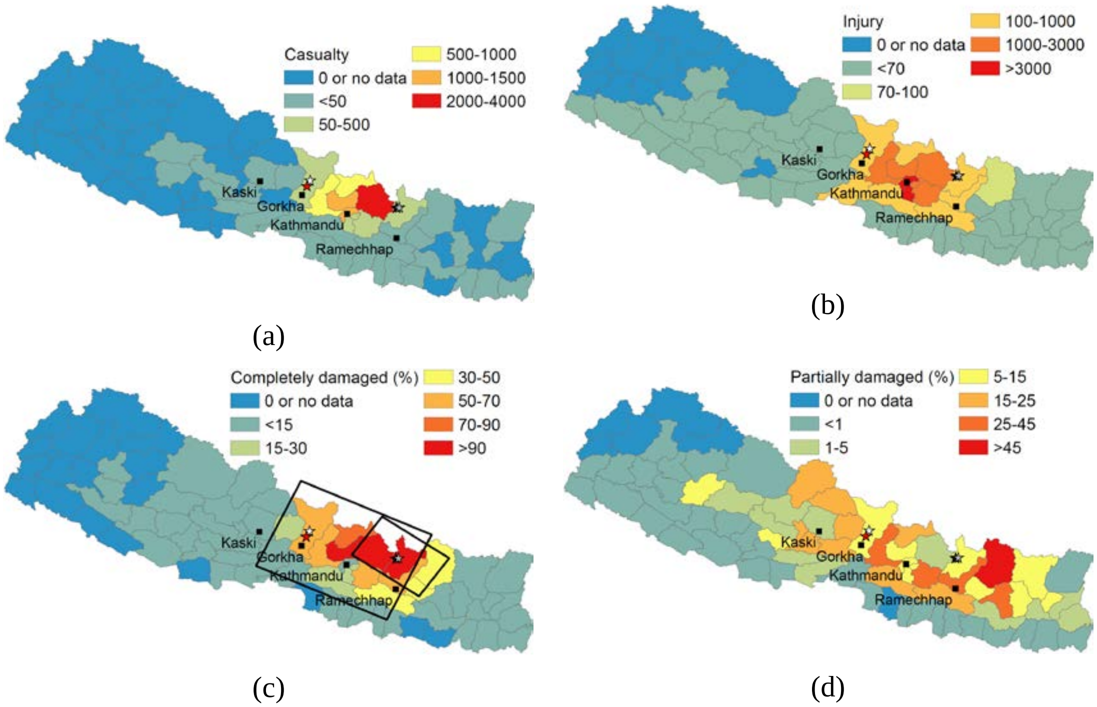

Fig. 1 –. Spatial distribution of (a) casualties (b) injuries (c) percentage of buildings completely damaged and (d) percentage of buildings partially damaged, caused by the 2015 Gorkha Earthquake and its aftershocks. The epicentres of the mainshock (Mw 7.6) estimated by USGS (red star) and NSC (white star) lie next to Gorkha. The epicentres of the largest aftershock (Mw 7.3) estimated by USGS (black star) and NSC (grey star) are east of Kathmandu and in the border region of Dolakha and Sindhupalchok districts. The black rectangles in (c) indicate the fault planes of the 25 April mainshock and the 12 May aftershock as estimated by USGS.

To investigate the relationship between the two scales, list of earthquakes with local magnitude greater than 4 were obtained from NSC. Data reported by USGS was downloaded from the USGS NEIC catalogue (http://earthquake.usgs.gov/earthquakes/search/). Events between 25 April 2015 and 18 June 2015 are considered. The USGS catalogue reports smaller events in body wave magnitude Mb. For earthquakes smaller than magnitude 5, Mb is assumed to be equal to Mw. Common events reported both by the USGS and NSC are then selected to study their relationship. In total, 121 events are obtained.

The results are shown in Fig. 3. The results show that the local magnitude is, on the average, larger than moment magnitude for smaller events (magnitude less than about 6). This is in contradiction to the general observation that between magnitude 4 and 6, the two scales yield approximately the same value (see, for example, [5]). For larger events, magnitude values in the two scales seem to be approximately the same (local magnitude only slightly smaller than moment magnitude). This is also in contradiction to the generally observed saturation of local magnitude around 6.9 (see, for example, [5]). It is rare to have local magnitude larger than 6.9: we are aware of only two such events, the 1976 Tangshan Earthquake with local magnitude ~7.5 and the 1940 Vrancea, Romania Earthuqake with local magnitude ~7.7 (see, for example, [6]). The local magnitude reported by the NSC does not seem to saturate.

It is interesting to note that the best fit line (green line in Fig. 2) matches the mainshock (see red star in Fig. 2) magnitude very well. However, the local magnitude of the 12 May aftershock (see blue star in Fig. 2) is smaller than what would be implied by the best fit line. The local magnitude of this aftershock was reported as 6.8, which would fit better with a local magnitude scale saturating around 6.9, as is generally reported in the literature. The model used by [7] to relate the local magnitude of earthquakes in Nepal to moment magnitude is shown by the red line in Fig. 2. This model, which has been calibrated for earthquakes smaller than magnitude 5, predicts a higher ratio between the two magnitude scales than is implied by the best fit line. In general, the data in Fig. 2 seem to fit a model where local magnitude is almost equal to moment magnitude for smaller events but saturates around 6.9, except for the 25 April mainshock with a reported local magnitude of 7.6.

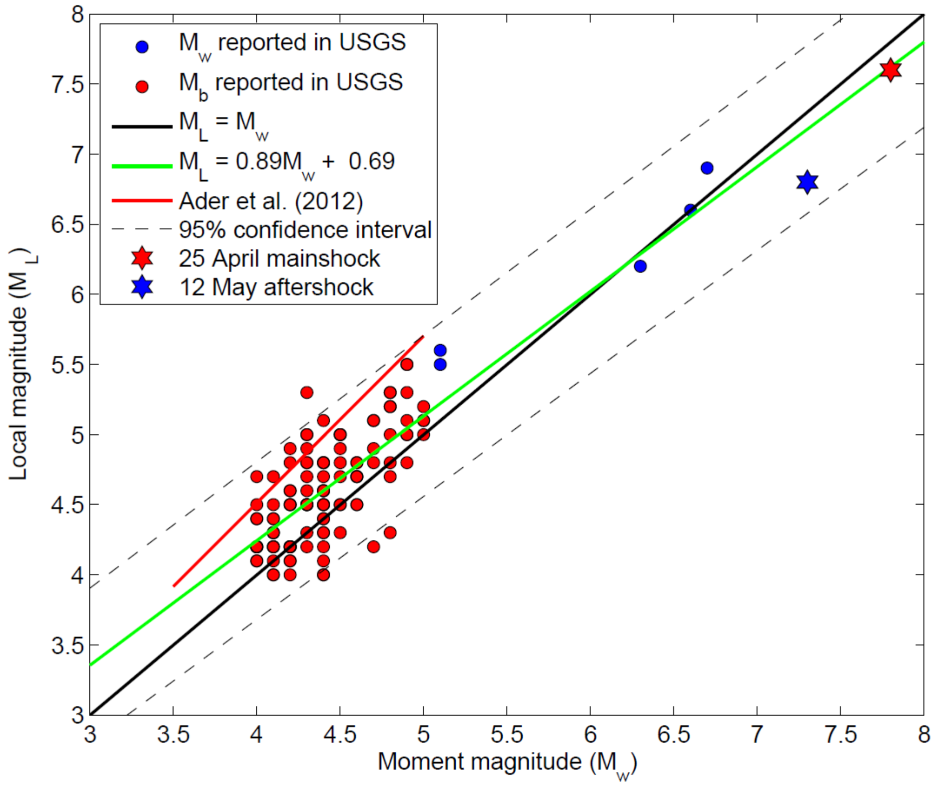

Fig. 2 – Relation between M_L reported by NSC and M_w reported by USGS of the 2015 Gorkha Earthquake and its aftershocks until 18 June 2015. The red dots represent the events for which USGS reports body wave magnitude, which are considered in this study to be equal to moment magnitude, while M_w is reported for the events plotted as blue dots. The green line is the best fit line obtained by least squares regression with its 95% confidence bounds represented by the dashed black lines. The equation of the regression line is shown in the legend. The red line is the model used by [7]. The red and the blue stars represent the 25 April mainshock and the 12 May aftershock, respectively.

3. Strong ground motion

In this section, some important characteristics of strong ground motion of the mainshock and some of the largest aftershocks are discussed. The only published strong motion data of the 25 April mainshock is the one from the Kantipath (KATNP) station of the USGS, which can be downloaded from the Centre for Engineering Strong Motion Data (CESMD).

3.1 Ground motion due to the mainshock

Ground motion recorded at KATNP during the 25 April mainshock is shown in Fig. 3. Ground acceleration, velocity, and displacement shown in the figure are obtained by baseline correction of the raw acceleration data provided by CESMD. The baseline correction method applied is the one described in [8], and no other processing has been applied to the data. The results indicate large permanent displacements (see values in the bottom row plots of Fig. 3). The coseismic displacements estimated from the ground motion data is larger than that reported from 5 Hz GPS data at Caltech Tectonic Observatory station NAST (see Fig. 4) as reported in [9].

Despite the discrepancy in the coseismic offsets, the waveforms of displacement at NAST (from GPS data) and KATNP (from strong-motion data) are remarkably similar. The static displacement seems to have occurred in about 5s (see bottom right plot in Fig. 3). This time is an indication of rise time, and is as reported in [9]. The displacement at bedrock station KKN4 (see Fig. 4) just north of Kathmandu is also reported in [9].

The peak value of horizontal ground acceleration is about 16% of acceleration due to gravity. This peak ground acceleration is relatively low for such a large magnitude earthquake, especially as the rupture surface lies directly beneath the recording station. The peak vertical acceleration is slightly higher at 19% of acceleration due to gravity. The horizontal components seem to be richer in long-period energy than the vertical component, while the vertical component seems to be richer in high frequency energy. A consequence of this is the higher peak ground acceleration in vertical components, but higher peak ground velocity in the horizontal components.

Although the peak ground acceleration in the vertical component is larger, the horizontal components are more energetic: the root mean squared (rms) acceleration during the strong motion phase (taken as the interval between 5% and 95% of first invariant of Arias Intensity tensor; see for example, [10]) in the east-west, north-south, and vertical directions are 0.04 g, 0.04g, and 0.03g, respectively

The higher energy content in horizontal components, despite lower peak acceleration values, is also obvious from Arias Intensity of the three components shown in Fig. 4. The intensity seems to build up faster and until longer in the horizontal components than in the vertical one. The vertical component has much lower Arias Intensity than the horizontal ones. There seems to be a rapid build-up of Arias Intensity around 66s (see the red curve in Fig. 5), which is due to the arrival of a strong phase around this time (see, North-South acceleration plot in Fig. 3). This could be the contribution of seismic waves generated by a strong asperity just north of Kathmandu (see, the fault rupture area shown in Fig. 4).

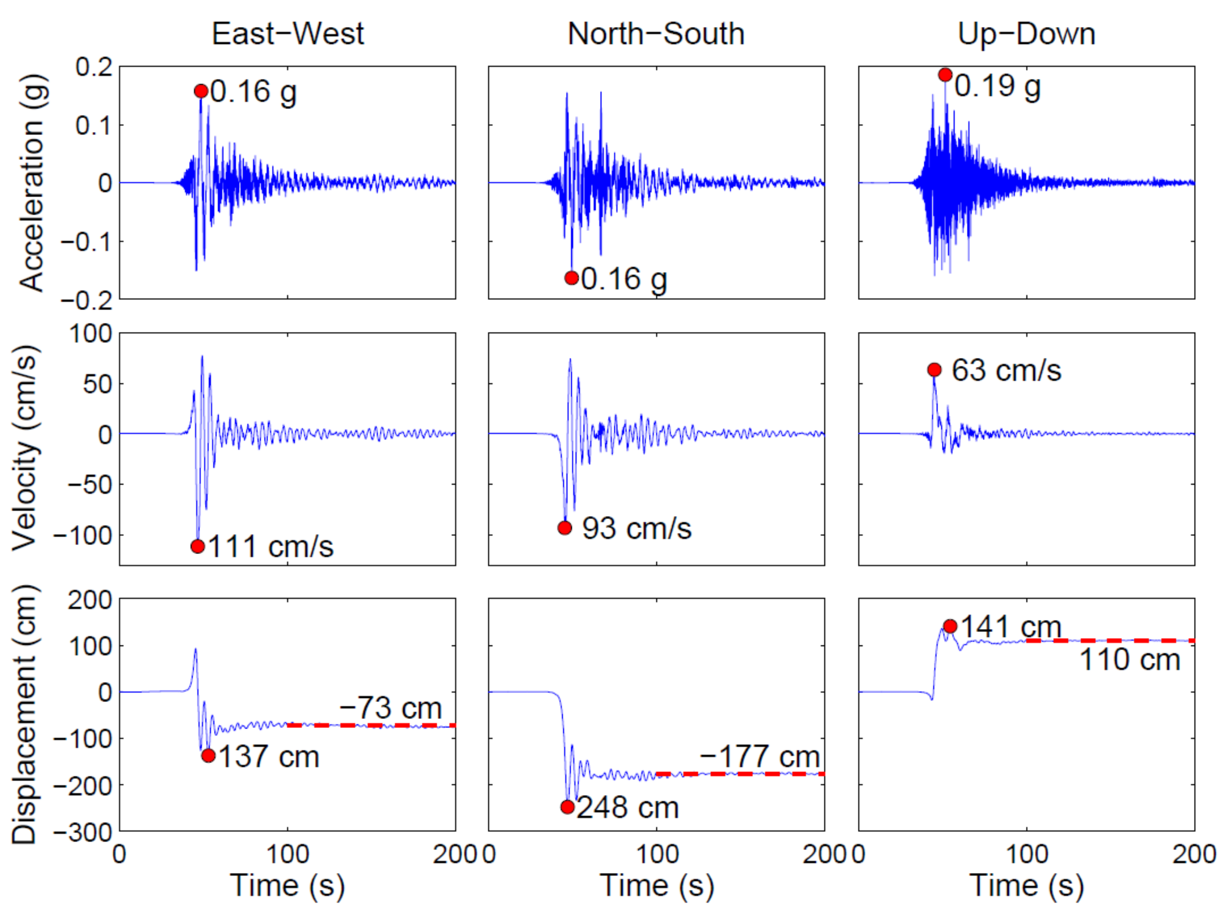

Fig. 3 – Acceleration, velocity, and displacement time histories at KATNP station during the 25 April mainshock.

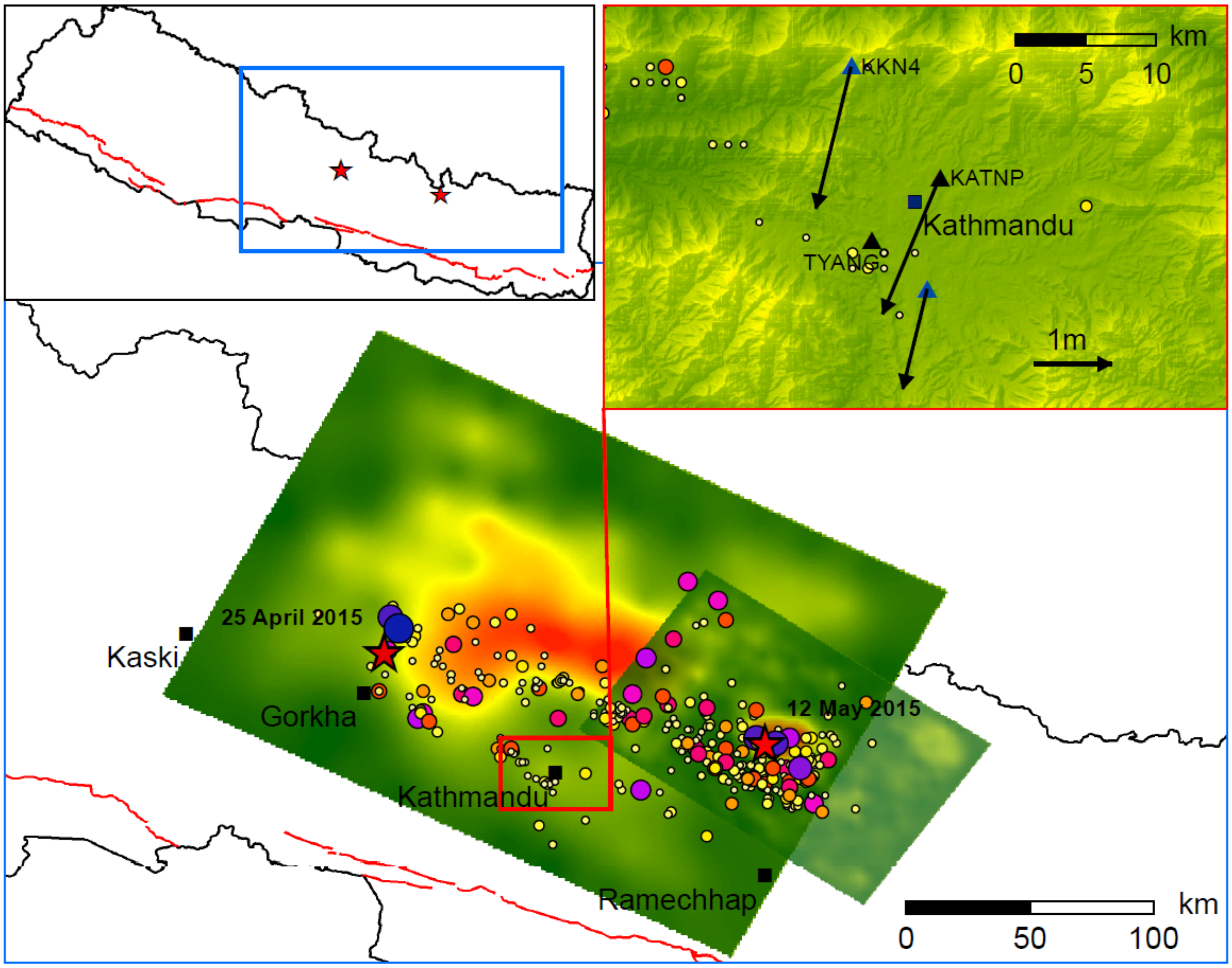

Fig. 4 – Top left: Map of Nepal showing the epicenter of the 25 April mainshock and the 12 May aftershock, the blue rectangle locates the area shown in the main figure. Main figure: the epicentral area of the Gorkha Earthquake and its aftershocks. The epicenter of the mainshock and the largest aftershock are marked with red stars (from USGS). The rectangles with filled color represent the fault planes of the two events (according to USGS) with the colors from green to red representing slip from 0 to 3m. The circles represent aftershocks between 25 April and 18 June taken from NSC, their size is scaled with earthquake magnitude. The red rectangle represents the area around Kathmandu Valley, which is shown in detail in the inset map on top right. Top right: Area around Kathmandu showing the strong-motion station of USGS (KATNP), that installed by EERC (TYANG), and the GPS stations operated by Caltech Tectonic Observatory (NAST and KKN4). Station KKN4 lies on bedrock while NAST lies on the sedimentary layers of Kathmandu basin. The black arrows indicate horizontal coseismic displacement vectors associated with the 25 April mainshock; those at KKN4 and NAST are estimated from GPS data [9] and the one at KATNP is estimated from strong-motion data using baseline correction method of [8].

The response spectra at KATNP station are compared with the Eurocode 8 (EC8) response spectra in Fig. 6. For the horizontal direction, rotation-invariant measure of spectrum [13] is used. The EC8 spectrum shown here corresponds to site class D and is scaled with rotation-invariant peak ground acceleration at KATNP station. The green curve in the left panel of Fig. 6 represents (approximately) the 475 year return period spectrum reported in [11]. It can be noted that the EC8 spectral shape fails to model the long-period peak of the recorded response spectra. Even the peak around 0.4s in the horizontal response spectrum is underestimated by the EC8 spectra. The spectra reported in [11] seem to over-estimate response below about 0.4s and under-estimate it at longer periods. The EC8 vertical response spectrum models the peak in the recorded spectra, but fails to model the long-period amplitudes.

Most of the buildings in Kathmandu are relatively short with fundamental period of vibration less than 1s (see, for example, [12]). These structures are thus not expected to be affected by the long period spectral amplitudes. On the other hand, some relatively tall buildings (for example, the 17-storey Park View Horizon apartment building) can be expected to have fundamental vibration period in the range of 1.5s to 2.5s, where the spectral ordinates of recorded motion is significantly higher than what is inferred from the EC8 model or the results of [11]. Such taller buildings suffered significant damage to infill walls. It should be noted that the ground shaking at high frequency during the 25 April mainshock is smaller than what can be expected for an event like this.

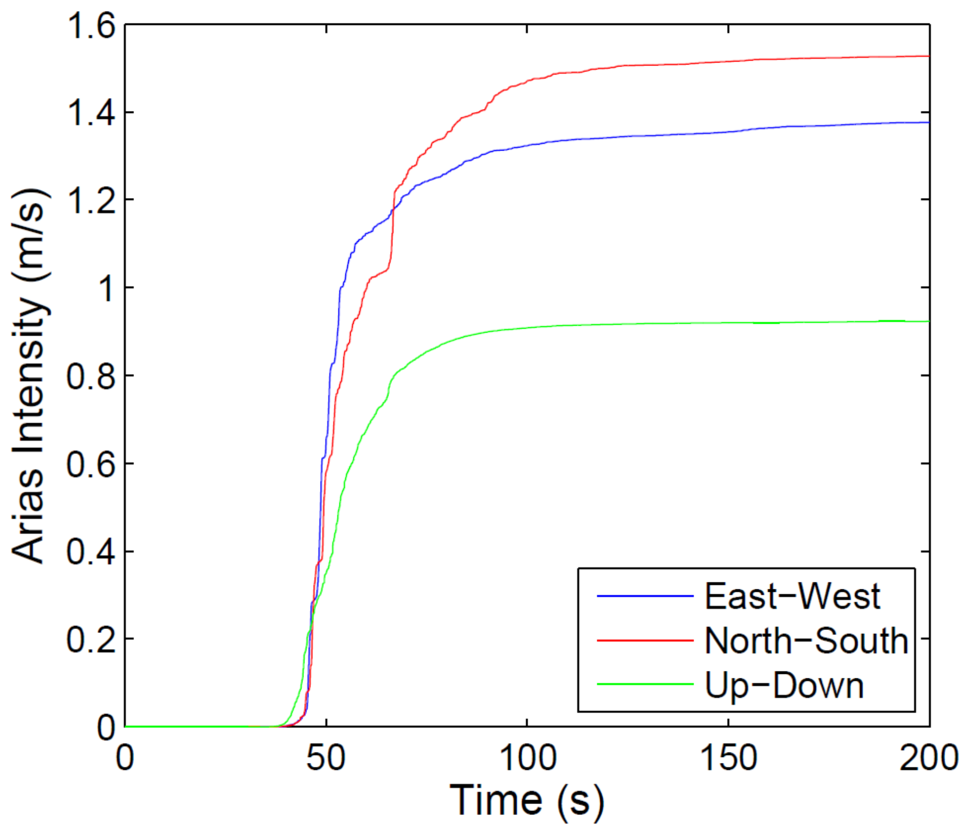

Fig. 5 – Time evolution of Arias Intensity of ground motion at KATNP during the 25 April mainshock.

3.2 Ground motion due to the aftershocks

This section discusses the characteristics of ground motion at KATNP due to the aftershocks of the 2015 Gorkha Earthquake. In total, ground motions due to eight aftershocks are discussed. Important information about the aftershocks, along with the mainshock are presented in Table 1.

The spectral shapes (pseudo-spectral acceleration normalized by the peak ground acceleration) of the mainshock and aftershocks recorded at KATNP station are shown in Fig. 7. The horizontal spectral shapes shown in Fig. 7 correspond to rotation-invariant response spectra. It can be noticed that significant variability exists in the spectral shapes of the aftershocks. The mean spectral shape of the aftershocks is similar to that of the mainshock at periods of vibration below ~1s. The amplitude of horizontal spectral shape of the mainshock is much larger than that of the mean of aftershocks at periods above ~1s. The distinct peak at ~5s which is observed in the spectral shape of the mainshock is missing from that of the aftershocks.

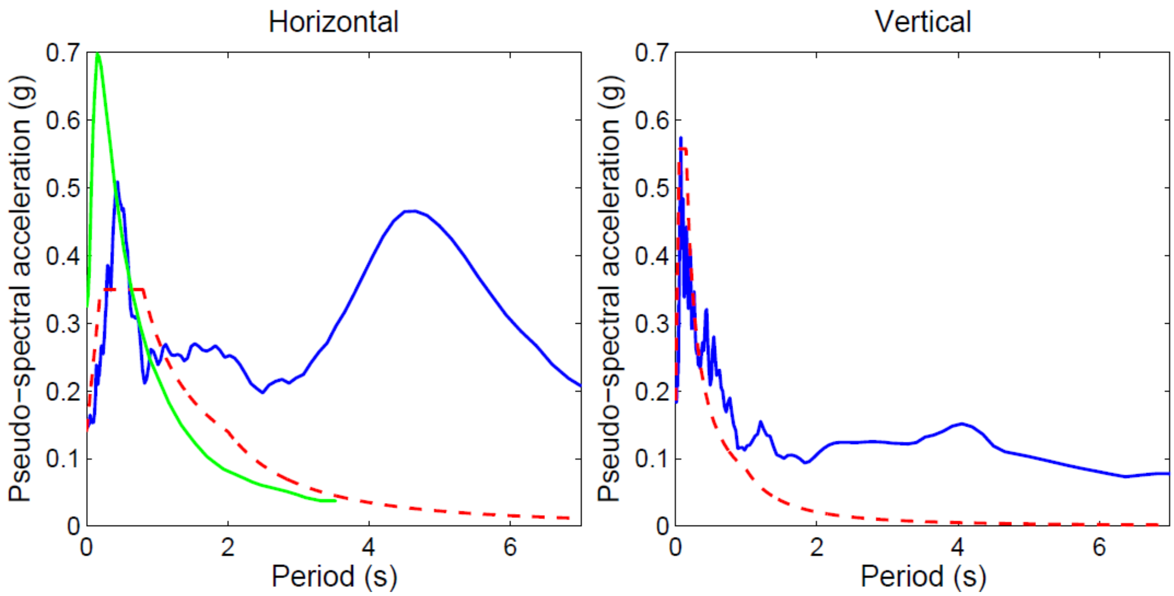

Fig. 6 – Comparison of 5% damped response spectrum with the Eurocode 8 (EC8) spectrum. The EC8 spectra are scaled with the rotation invariant measures of peak ground acceleration (see, [13]). For the horizontal direction, the 475 year return period response spectrum reported in [11] is shown with the green curve.

Table 1 – Important characteristics of ground motion due to the 2015 Gorkha Earthquake and its aftershocks at KATNP station.

Event	Date (dd/mm)	Time (hh:mm:ss, GMT)	Latitude (°, USGS)	Longitude (°, USGS)	M_w (USGS)	R (km)[1]	PGA_h (g)[2]	PGA_v (g)[3]
1	25/04	06:11:26	28.15	84.71	7.8	76.9	0.132	0.186
2	25/04	06:45:21	28.21	84.82	6.6	74.2	0.057	0.045
3	25/04	06:56:05	27.88	85.75	5.5	46.7	0.025	0.005
4	25/04	08:55:56	27.59	85.51	5.3	23.3	0.066	0.072
5	25/04	23:16:15	27.80	84.87	5.1	44.8	0.052	0.013
6	26/04	07:09:10	27.77	86.02	6.7	69.3	0.069	0.039
7	26/04	16:26:05	27.76	85.77	5.3	45.0	0.016	0.003
8	12/05	07:05:19	27.82	86.08	7.3	76.1	0.085	0.075
9	12/05	07:36:53	27.61	86.17	6.3	85.1	0.027	0.009

[1] Epicentral distance based on the location reported by USGS

[2] Rotation-invariant peak horizontal ground acceleration

[3] Peak vertical ground acceleration

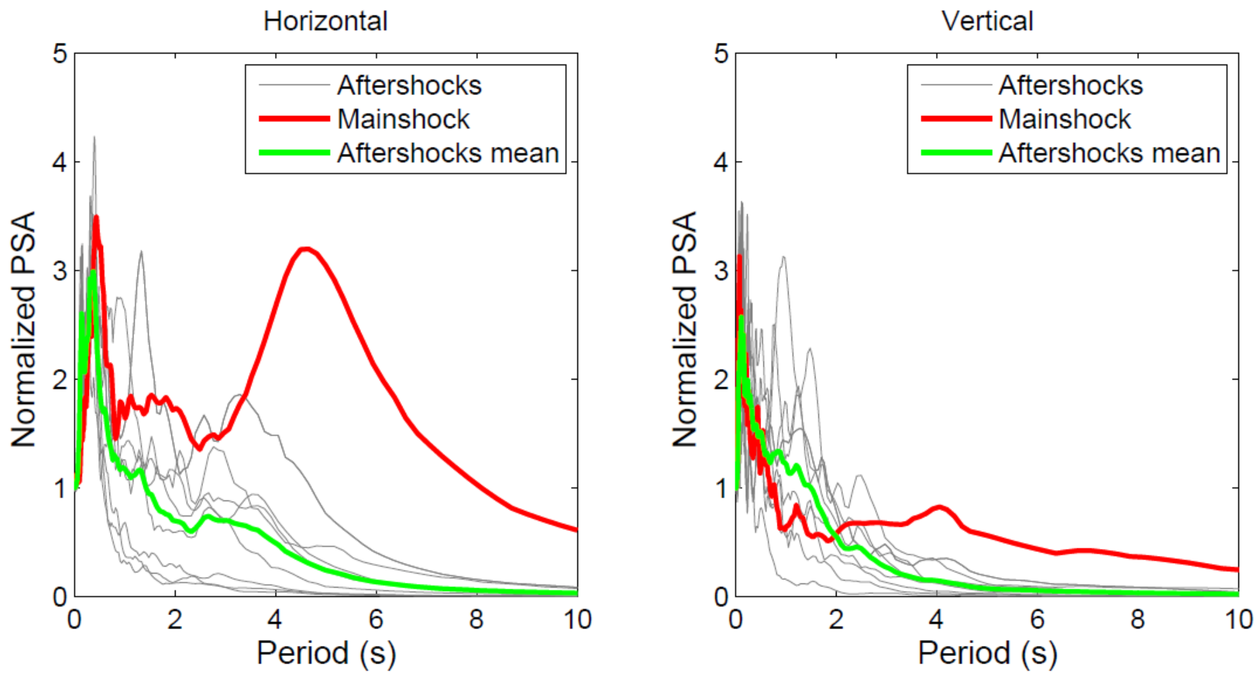

Fig. 7 – Pseudo-spectral acceleration (5% damped PSA) normalized by peak ground acceleration (PGA) of the 25 April mainshock and its aftershocks (see Table 1) recorded at KATNP station.

The spectral shape of the mainshock and the mean spectral shapes of the aftershocks with Mw greater than 6 are compared with EC8 Type 1 spectral shape for site class D in Fig. 8. The spectral shape inferred from the 475 year return period spectra reported in [11] is also shown for horizontal ground motion. For horizontal motion, the EC8 spectral shape captures the overall shape of the response spectra of the mainshock upto a vibration period of ~1s and that of the aftershocks up to a vibration period of ~2s. However, it under-estimates the peak amplitude of the spectral shape significantly. The spectral shape inferred from 475 year return period response spectrum reported in [11] fails to capture the spectral shape of the mainshock as well as the aftershocks. For vertical motion, the EC8 spectral shape over-estimates spectral ordinates at short periods and under-estimates them at long periods (above ~ 0.2s). These results indicate that the source and the site effects during the mainshock and the aftershocks are not appropriately modelled by standard spectral shapes used in modern design codes.

4. Conclusions

The 2015 Gorkha Earthquake sequence was a major disaster in Nepal, causing widespread damage. It killed several thousand people, and many more injured. Close to a million houses were affected, many of them completely collapsed, leaving many people without shelter. It also caused a significant damage to the economy of the country. This is the first large earthquake for which strong ground motion data have been recorded in Nepal. Unfortunately, strong motion monitoring network is not well developed in the country, and the only data that has been publicly released are from a single station operated by USGA in KATNP station in Kathmandu. Strong-motion at a nearby station were recorded by NSC, but unfortunately, the data has not been publicly released yet.

Ground motion recorded in KATNP during the mainshock of 25 April are peculiar in many aspects. The horizontal PGA recorded at this station was rather low for an earthquake of this size, considering the fact that Kathmandu lies right on top of the rupture surface. On closer inspection, it can be noticed that, although the horizontal PGA which is governed by high-frequency contents is relatively low, energy content at low frequencies is unusually high. Response spectral ordinates at periods close to 5s are close to 0.5g which is very unusual. This long-period energy content is due to the source effect which radiated relatively long-period waves combined with the site effects caused by the deep sedimentary basin of Kathmandu Valley. It is interesting to note that the vertical PGA is larger than the horizontal, which is also not very common. However, the overall energy content, characterized by root mean square acceleration as well as Arias Intensity, are much larger in the horizontal directions than in the vertical direction. This implies less energetic but peakier motion in the vertical direction than in the horizontal. Vertical component of motion was observed to be richer in higher frequencies than the horizontal components of motion, and vice versa at lower frequencies. Elastic response spectral shapes of horizontal motion were significantly larger, at vibration periods longer than about 1s, than those implied by modern design codes such as the EC8. Uniform hazard spectra at 475 mean return period based on attenuation equations calibrated from data recorded elsewhere failed to capture the elastic response spectral shapes of both the mainshock and the largest aftershocks. Although a significant peak in elastic response spectra is observed at a period close to 5s in the horizontal motion of the mainshock, the aftershocks lack this feature. Even in the lack of this peculiar effect in aftershock motion, response spectral shapes based on EC8 as well as uniform hazard spectra based on probabilistic seismic hazard assessment fail to capture the spectral content of ground motion. This is a very important consideration for seismic resistant design of structures, especially those with fundamental vibration period longer than about 0.5s in Kathmandu Valley. It is apparent that use of standard response spectral shapes may significantly underestimate seismic action on such structures in the valley. This points to the need for proper ground motion models and geotechnical site response models for estimating suitable seismic design actions. To achieve this strong ground motion monitoring needs to expanded and modernized significantly. In addition, detailed geotechnical investigation and site response analysis needs to be conducted, with focus on not only the effects of superficial soil layers but also basin and topographic effects.

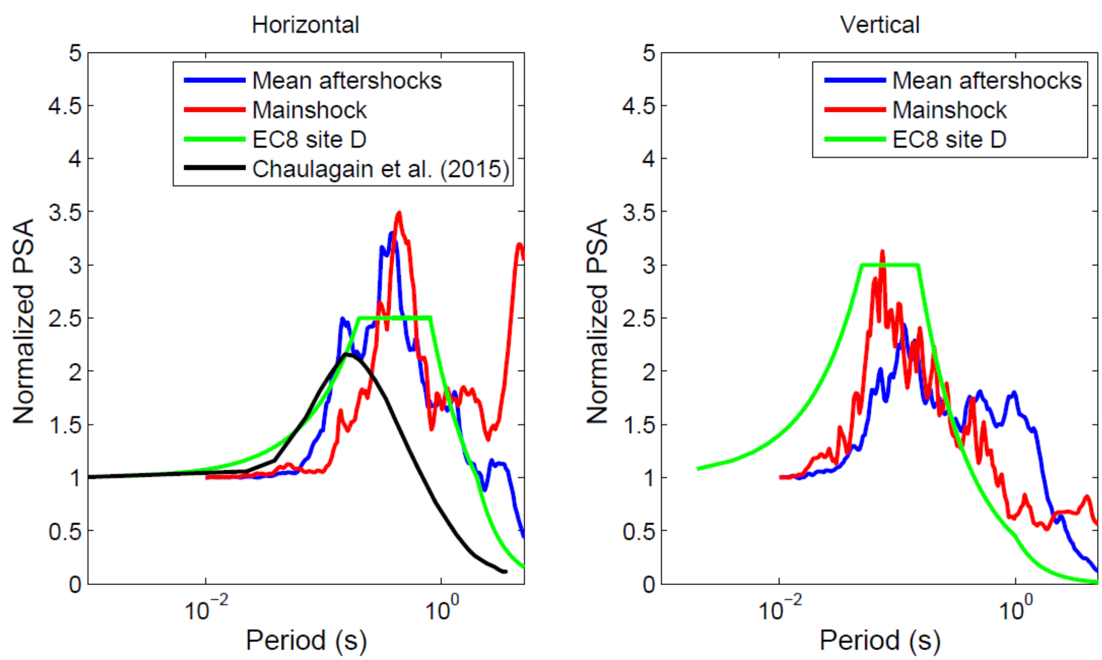

Fig. 8 – Pseudo-spectral acceleration (5% damped PSA) normalized by peak ground acceleration (PGA) of the 25 April mainshock and its aftershocks recorded at KATNP compared with the Type 1 EC8 site class D spectral shapes and that of [11]. The mean spectral shape of aftershocks is obtained from events with Mw greater than 6 to make a meaningful comparison with EC8 Type 1 spectral shape. Note that the horizontal axis in is logarithmic scale.

5. Acknowledgements

We acknowledge financial support from the University of Iceland Research Fund and the National Power Company of Iceland, Landsvirkjun.

6. References

[1] United States Geological Survey (USGS) (2015), http://earthquake.usgs.gov/earthquakes/eventpage/us20002926#general_summary (last accessed 21 June 2015)

[2] National Seismological Centre (NSC) http://www.seismonepal.gov.np/ (last accessed 21 June 2015)

[3] Ekström G, Nettle M, Dziewonski AM (2012): The global CMT project 2004-2010: Centroid-moment tensors for 13,107 earthquakes. *Phys. Earth Planet. Inter.*, **200-201**:1-9

[4] Nepal Earthquake 2015: Disaster relief and recovery information platform (NDRRIP), Nepal Diasaster Risk Reduction Portal, http://drrportal.gov.np/ (last accessed 21 June 2015)

[5] Kanamori H (1983): Magnitude scale and quantification of earthquakes. In: Dutta S J and Aki K (editors), *Quantification of Earthquakes*, *Tectonophysics*, **93**:185-199

[6] Lay T, Wallace TC (1995): *Modern Global Seismology*. Academic Press

[7] Ader T, Avouc J-P, Liu-Zeng J, Lyon-Caen H, Bollinger L, Galetzka J, Genrich J, Thomas M, Chanard K, Sapkota S N, Rajaure S, Shrestha P, Ding L, Flouzat M (2012): Convergence rate across the Nepal Himalaya and interseismic coupling on the Main Himalayan Thrust: Implications for seismic hazard. *Journal of Geophysical Research*, **117**(B04403):1-16

[8] Rupakhety R, Halldorsson B, Sigbjörnsson R (2010): Estimating coseismic deformations from near source strong motion records: methods and case studies. *Bulletin of Earthquake Engineering*, **8**(4): 787-811

[9] Galetzka J, Melgar D, Genrich JF, Geng J, Owen S, Lindsey EO, Xu X, Bock Y, Avouac JP, Adhikari LB, Upreti BN (2015): Slip pulse and resonance of the Kathmandu basin during the 2015 Gorkha earthquake, Nepal. *Science*, **349**(6252):1091-5.

[10] Rupakhety R, Sigbjörnsson R (2014): Three-dimensional characteristics of strong-ground motion in the near-fault area. In *Proceedings of the Second European Conference on Earthquake Engineering and Seismology*, 25-29 Aug 2014, Istanbul

[11] Chaulagain H, Rodrigues H, Silva V, Spacone E, Varum H (2015) Seismic risk assessment and hazard mapping in Nepal. *Natural Hazards*, DOI 10.1007/s11069-015-1734-6

[12] Chaulagain H, Rodrigues H, Spacone E, Varum H (2015) Seismic response of current RC buildings in Kathmandu Valley. *Structural Engineering Mechanics*, **52**:791-818

[13] Rupakhety R, Sigbjörnsson R (2013): Rotation-invariant measures of earthquake response spectra. *Bulletin of Earthquake Engineering*, **11**(6):1885-93.